Hard X-ray view of the γ-ray binary LS I +61°303

E.A. Saavedra[1] & G.E. Romero[1,2]

[1] *Facultad de Ciencias Astronómicas y Geofísicas, UNLP, Argentina*
[2] *Instituto Argentino de Radioastronomía, CONICET–CICPBA–UNLP, Argentina*

Contact / saavedraenz@gmail.com

Resumen / En este trabajo presentamos los resultados de un estudio de la emisión de rayos X de la fuente LS I +61°303 detectada por el satélite *NuSTAR*. La observación se realizó el 14 de agosto de 2017 y tiene una duración de 55 ks. La curva de luz en el rango de energía de 3 a 79 keV está dominada por una emisión persistente de $\sim$ 0,5 c/s, para un bin de 5 s. Esta emisión se superpuso a dos microllamaradas con una intensidad máxima de 1.5 c/s. El análisis espectral mostró que un modelo de ley de potencia absorbida es suficiente para describir el espectro. El índice de ley de potencia ($E^{-\Gamma}$) fue de $\sim$ 2. Describimos brevemente el escenario físico en el que puede producirse esta emisión.

Abstract / In this paper, we present the results of a study of the X-ray emission of the source LS I +61°303 detected by the *NuSTAR* satellite. The observation was made on August 14, 2017, with an exposure of 55 ks. The lightcurve in the energy range from 3 to 79 keV is dominated by persistent emission of $\sim$ 0.5 c/s, for a bin of 5 s. Superposed to this emission, two microflares were detected with a maximum intensity of 1.5 c/s. Spectral analysis showed that an absorbed power law is sufficient to describe the spectrum. The power law index ($E^{-\Gamma}$) was 2. We briefly describe a physical scenario where this emission can occur.

Keywords / X-rays: binaries — stars: neutron

1. Introduction

The number of binary systems where high-energy (HE; 0.1-100 GeV) and/or very high-energy (VHE; $>$ 0.1 TeV) γ-ray emission has been detected is small. These systems, however, are important for studying particle acceleration because they harbor all the ingredients that accelerate particles up to relativistic energies on short timescales and because of their relative proximity.

In the last few decades, several types of HE emitting binary systems have been discovered, including three high-mass X-ray binaries (Cyg X-1, Cyg X-3, and SS 433), several neutron-star/low-mass star binaries, two colliding wind binaries (η-Car and WR11), and six gamma-ray binaries. Only the gamma-ray binaries display significant VHE emission (Dubus, 2013, 2015).

A high-mass X-ray binary, LS I +61 303, is a system consisting of a B0 Ve star (Casares et al., 2005) and a compact object whose nature has remained unknown for decades (Romero et al., 2007, 2008). The system is located at a distance of 2.0±0.2 kpc according to HI measurements (Frail & Hjellming, 1991). Very recently, the detection of radio pulses has provided evidence supporting that the compact object is a rotating neutron star (NS), rather than a black hole (Weng et al., 2022). This discovery sheds new light on the nature of the system and has important implications for our understanding of high-mass X-ray binaries.

The observed modulation of the radio emission with a period of 26.496±0.003 days corresponds to the binary orbital period (Taylor & Gregory, 1982). The nonthermal X-ray emission of LS I +61 303 is also modulated with the orbit and exhibits outbursts between orbital phases 0.4 and 0.8 (Li et al., 2012; Abdo et al., 2009; Zamanov et al., 2014).

Mestre et al. (2022) found that LS I +61 303 exhibits optical microflares with timescales of one day, and that these microflares are correlated with gamma-ray emission. It has been repeatedly suggested that the compact object may be a magnetar, i.e. a neutron star with a magnetic field greater than 14 G (Torres et al., 2012; Zamanov et al., 2014; Suvorov & Glampedakis, 2022).

2. Observation and Data Analysis

2.1. *Swift*/BAT data

NASA launched the *Swift* satellite in 2004, which includes *Swift Burst Alert Telescope* (BAT) as part of its multiwavelength observatory (Gehrels et al., 2004). BAT uses a coded aperture mask to detect and locate gamma-ray bursts (GRBs) in the 15-150 keV energy range. Its wide field of view and high sensitivity allow it to provide initial positions for follow-up observations by other instruments on *Swift* satellite and ground-based telescopes in less than 20 seconds.

BAT has several technical capabilities that make it useful for a range of astronomical studies. Its large field of view allows it to survey a significant fraction of the sky each day, which is useful for studies of the cosmic X-ray background and the large-scale structure of the universe. Additionally, its good angular resolution enables it to accurately locate and study a variety of astronomical objects, such as active galactic nuclei, X-ray binaries, and supernova remnants (Barthelmy et al., 2005).

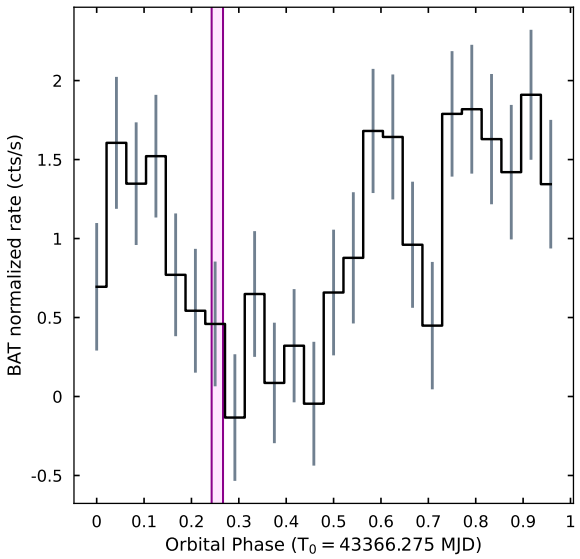

Figure 1: *Swift*/BAT folded light curve using 32 bins, an orbital period of 26.496 days and a reference epoch 43366.275 MJD (Gregory, 2002). The *NuSTAR* observation of LS I +61 303 used in this work is represented by the pink stripe, spanning ∼2.4% of the orbital period. The observation ranges from 0.242 – 0.266.

We consider the full orbital lightcurve of LS I +61 303 available on Swift/BAT service up to November 16, 2022. This public website* offers over 1000 lightcurves of hard X-ray sources, spanning over 9 years.

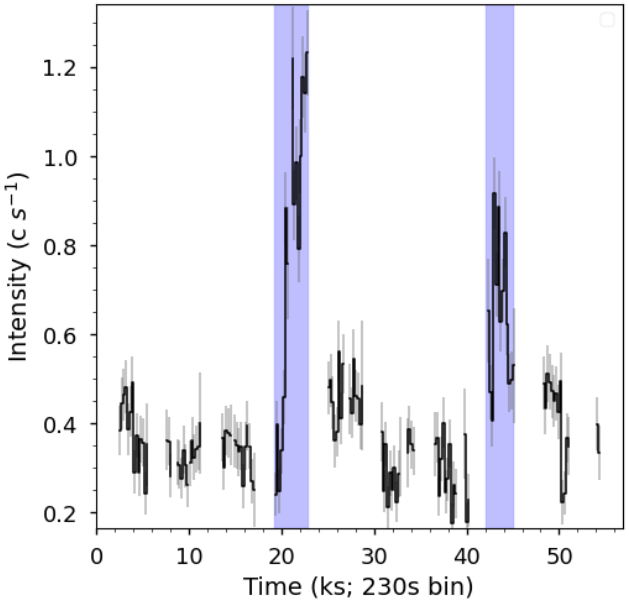

Figure 2: Background corrected lightcurve of LS I +61 303 with a binning of 230 s, starting at 55197.76601 MJD. Microflares can be identified in the red stripes. The errors associated with each count over second shown in gray.

*LS I +61 303

2.2. NuSTAR data

NuSTAR (*Nuclear Spectroscopic Telescope Array*; Harrison et al. 2013) was designed and launched to study high-energy X-rays. It is the first telescope with the ability to focus X-rays in the 3-79 keV energy range, providing a unique view of the universe. *NuSTAR* consists of two co-aligned telescopes with grazing incidence optics modules and focal plane modules, A (*FPMA*) and B (*FPMB*), consisting of a solid-state CdZnTe solid-state detector.

NuSTAR also has technical capabilities that make it useful for a wide range of scientific studies. *NuSTAR* has a good angular resolution, with a point spread function that varies from 18 arcsec at 10 keV to 58 arcsec at 79 keV, which allows for detecting these spectral features with high-efficiency (Fürst et al., 2014; Saavedra et al., 2022a, 2023). This allows *NuSTAR* to accurately locate and study various astronomical objects. *NuSTAR* also has a good energy resolution, with a FWHM of 350 eV at 10 keV and 900 eV at 79 keV. This enables *NuSTAR* to measure the energies of incoming X-rays with high precision (see for e.g, Saavedra et al., 2021, 2022b).

NuSTAR observed LS I +61 303 on August 14, 2017 (ObsID 90301008002), with an exposure of ∼ 55 ks. The data were reduced using `NuSTARDAS-v. 2.0.0` analysis software from the `HEASoft` v.6.28 task package and `CALDB` (V.1.0.2) calibration files.

In order to filter the Southern Atlantic Anomaly (SAA) passages, we looked at the individual observation report. We extracted cleaned event files using `saacalc=1`, `saamode=OPTIMIZED` and `tentacle=NO` parameters.

To extract the photons, we used circular regions of 70 arcsec centered at the centroid of the source and of 70 arcsec for the background, using the same chip. The chosen radius encloses ∼ 90% of the point spread function (PSF). The background subtraction of each camera module and the addition of corrected lightcurves were done using the LCMATH task.

To generate the spectra, we used the `nuproducts` task with the same regions as for lightcurve extraction. The X-ray spectral analysis was performed using `xspec` v.12.12.1 (Arnaud, 1996) in the 3-79 keV energy range. The spectra were grouped to a minimum of 25 counts per bin to properly use χ^2 statistics.

3. Results

In Figure 1 we show the *NuSTAR* observation in terms of the orbital phase given by Swift/BAT. The observation is in the phase from 0.242 – 0.266. This was coincident with passage through the periastron where high activity at different wavelengths was observed.

In Figure 2 we show the *NuSTAR* lightcurve with a time bin of 230 s. In it, we identify two microflares that are approximately 3 times higher than the persistent emission. The initial microflare lasted for ∼ 5.9 ks, whereas the second one lasted for ∼ 7.9 ks.

Motivated to understand the nature of the microflares, we obtained spectra of the persistent emission

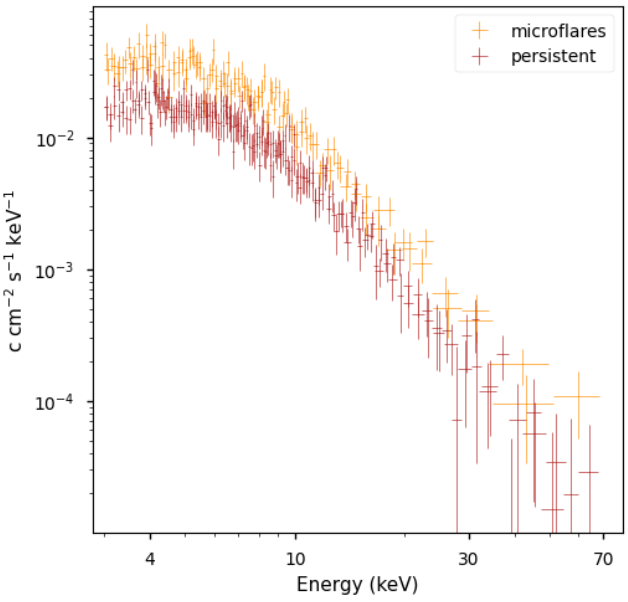

Figure 3: The energy spectra of LS I +61 303 observed by FPMA and FPMB show persistent emission and emission associated with microflares that can be characterized by an absorbed power-law contribution in the energy range 3-79 keV.

and the microflares. Figure 3 shows the associated spectra.

We fitted both spectra with an absorbed power law (in `xspec`: `tbabs*powerlaw`). The absorption column could not be correctly constrained at energies above 3 keV so it was fixed at 0.77×10^{22} cm^{-2} derived from the HEASARC NH web tool **. This model gave us a very good fit. For the average spectrum of the persistent emission, $\Gamma = 2.00 \pm 0.05$ with $\chi^2/d.o.f = 115/125$. For the average spectrum of the microflares, $\Gamma = 2.10 \pm 0.07$ with $\chi^2/d.o.f$ equal to 198/225. These results are consistent with a $\Gamma \sim 2$.We obtained the flux associated with the `cflux` model in the 3-79 keV range. The parameters can be seen in Table 1.

Table 1: Parameters associated with the models fitted to the spectra. † The flux is in units of 10^{-11} erg s^{-1} cm^{-2}

	persistent	microflares
nH [10^{22} cm^{-2}]	0.77	0.77
Γ	2.00 ± 0.05	2.10 ± 0.07
Norm [10^3]	2.1 ± 0.2	4.3 ± 0.2
Flux†	0.73 ± 0.01	1.96 ± 0.05
χ^2/d.o.f	115/125	198/225

**https://heasarc.gsfc.nasa.gov/cgi-bin/Tools/w3nh/w3nh.pl

4. Discussion and conclusions

We identified two microflares in the LS I +61 303 lightcurve. If we assume that the source is at $\sim$ 2 kpc, the luminosity associated with the persistent emission was $\sim 3.52\times10^{33}$ erg s^{-1}, while the luminosity associated with the microflares was $\sim 9.5\times10^{33}$ erg s^{-1}.

We do not rule out that X-ray microflares have a common origin with the gamma-ray and the optical emission, as suggested by Mestre et al. (2022). This would imply a common origin resulting from shocks generated in the pulsar wind. In this scenario most of the kinetic energy is dissipated in the form of X-rays generated by synchrotron mechanism as the shock moves through a turbulent medium. The radiation is then partially absorbed by the neutral gas ahead or behind the shock and re-emitted at lower frequencies (Metzger et al., 2014).

In the shocks, part of the gamma-ray emission, which is produced by Inverse Compton up-scattering of thermal photons, is not able to escape and is reprocessed contributing then to the radio up to optical output of the system. The shocked regions are expected to form naturally as the compact object's magnetosphere interacts with the circumstellar disk of the star Be.

Acknowledgements: EAS is a fellow of the Consejo Interuniversitario Nacional, Argentina. GER acknowledges support from PIP 0554 (CONICET) and by the Spanish Ministerio de Ciencia e Innovación (MICINN) under grant PID2019-105510GB-C31/AEI/10.13039/501100011033 and through the "Center of Excellence María de Maeztu 2020-2023" award to the ICCUB (CEX2019-000918-M).

References

Abdo A.A., et al., 2009, ApJL, 701, L123
Arnaud K.A., 1996, *ADASS V*, *ASPCS*, vol. 101, 17
Barthelmy S.D., et al., 2005, SSRv, 120, 143
Casares J., et al., 2005, MNRAS, 360, 1105
Dubus G., 2013, A&A Rv, 21, 64
Dubus G., 2015, Comptes Rendus Physique, 16, 661
Frail D.A., Hjellming R.M., 1991, AJ, 101, 2126
Fürst F., et al., 2014, ApJL, 784, L40
Gehrels N., et al., 2004, ApJ, 611, 1005
Gregory P.C., 2002, ApJ, 575, 427
Harrison F.A., et al., 2013, ApJ, 770, 103
Li J., et al., 2012, ApJL, 744, L13
Mestre E., et al., 2022, A&A, 662, A27
Metzger B.D., et al., 2014, MNRAS, 442, 713
Romero G.E., et al., 2007, A&A, 474, 15
Romero G.E., et al., 2008, Int. J. Mod. Phys. D, 17, 1875
Saavedra E.A., et al., 2021, BAAA, 62, 277
Saavedra E.A., et al., 2022a, A&A, 659, A48
Saavedra E.A., et al., 2022b, BAAA, 63, 274
Saavedra E.A., et al., 2023, arXiv e-prints, arXiv:2304.03130
Suvorov A.G., Glampedakis K., 2022, ApJ, 940, 128
Taylor A.R., Gregory P.C., 1982, ApJ, 255, 210
Torres D.F., et al., 2012, ApJ, 744, 106
Weng S.S., et al., 2022, Nat. Astron., 6, 698
Zamanov R., et al., 2014, A&A, 561, L2